American Mineralogist, Volume 97, pages 212–219, 2012

Lead-tellurium oxysalts from Otto Mountain near Baker, California: VII. Chromschieffelinite, $Pb_{10}Te_6O_{20}(OH)_{14}(CrO_4)(H_2O)_5$, the chromate analog of schieffelinite

Anthony R. Kampf,[1,*] Stuart J. Mills,[2] Robert M. Housley,[3] Michael S. Rumsey,[4] and John Spratt[4]

[1]Mineral Sciences Department, Natural History Museum of Los Angeles County, 900 Exposition Blvd., Los Angeles, California 90007, U.S.A.
[2]Geosciences, Museum Victoria, GPO Box 666, Melbourne 3001, Australia
[3]Division of Geological and Planetary Sciences, California Institute of Technology, Pasadena, California 91125, U.S.A.
[4]Mineralogy Department, Natural History Museum, Cromwell Road, London SW7 5BD, U.K.

Abstract

Chromschieffelinite, $Pb_{10}Te_6O_{20}(OH)_{14}(CrO_4)(H_2O)_5$, is a new tellurate from Otto Mountain near Baker, California, named as the chromate analog of schieffelinite, $Pb_{10}Te_6O_{20}(OH)_{14}(SO_4)(H_2O)_5$. The new mineral occurs in a single 1 mm vug in a quartz vein. Associated mineral species include: chalcopyrite, chrysocolla, galena, goethite, hematite, khinite, pyrite, and wulfenite. Chromschieffelinite is orthorhombic, space group $C222_1$, a = 9.6646(3), b = 19.4962(8), c = 10.5101(7) Å, V = 1980.33(17) Å^3, and Z = 2. Crystals are blocky to tabular on {010} with striations parallel to [001]. The forms observed are {010}, {210}, {120}, {150}, {180}, {212}, and {101}, and crystals reach 0.2 mm in maximum dimension. The color and streak are pale yellow and the luster is adamantine. The Mohs hardness is estimated at 2. The new mineral is brittle with irregular fracture and one perfect cleavage on {010}. The calculated density based on the ideal formula is 5.892 g/cm^3. Chromschieffelinite is biaxial (–) with indices of refraction α = 1.930(5), β = 1.960(5), and γ = 1.975(5), measured in white light. The measured $2V$ is 68(2)°, the dispersion is strong, $r < v$, and the optical orientation is X = **b**, Y = **c**, Z = **a**. No pleochroism was observed. Electron microprobe analysis provided: PbO 59.42, TeO_3 29.08, CrO_3 1.86, H_2O 6.63 (structure), total 96.99 wt%; the empirical formula (based on 6 Te) is $Pb_{9.65}Te_6O_{19.96}(OH)_{14.04}(CrO_4)_{0.67}(H_2O)_{6.32}$. The strongest powder X-ray diffraction lines are [d_{obs} in Å (*hkl*) *I*]: 9.814 (020) 100, 3.575 (042,202) 41, 3.347 (222) 44, 3.262 (241,060,113) 53, 3.052 (311) 45, 2.9455 (152,133) 55, 2.0396 (115,353) 33, and 1.6500 (multiple) 33. The crystal structures of schieffelinite (R_1 = 0.0282) and chromschieffelinite (R_1 = 0.0277) contain isolated $Te^{6+}O_6$ octahedra and $Te_2^{6+}O_{11}$ corner-sharing dimers, which are linked into a three-dimensional framework via bonds to Pb^{2+} atoms. The framework has large channels along **c**, which contain disordered SO_4 or CrO_4 groups and H_2O. The lone-electron pair of each Pb^{2+} is stereochemically active, resulting in one-sided Pb-O coordination arrangements. The short Pb-O bonds of the Pb^{2+} coordinations are all to $Te^{6+}O_6$ octahedra, resulting in strongly bonded layers parallel to {010}, which accounts for the perfect {010} cleavage.

Keywords: Chromschieffelinite, new mineral, tellurate, crystal structure, schieffelinite, Otto Mountain, California

Introduction

During our continuing investigations of new (Kampf et al. 2010a, 2010b, 2010c, 2010d, 2010e, 2010f) and unusual (Kampf et al. 2010g) secondary minerals from Otto Mountain, near Baker, California, John Dagenais of Vancouver, Canada, submitted a specimen that he had collected, which contained unknown pale yellow crystals. The crystals provided a powder X-ray diffraction (PXRD) pattern very similar to that reported by Williams (1980) for schieffelinite and provided semi-quantitative chemistry from energy-dispersive X-ray spectroscopy (EDS) that was reasonably consistent with schieffelinite, but with Cr instead of S. In his description of schieffelinite from the Joe and Grand Central mines, Tombstone, Arizona, Williams (1980) provided two "plausible" formulas, $Pb(Te,S)O_4 \cdot H_2O$ and $Pb_8(TeO_4)_5(SO_4)_3 \cdot 8H_2O$. To unambiguously determine the relationship between the unknown yellow crystals and schieffelinite, we undertook a reexamination of schieffelinite based upon cotype specimens in the collections of the U.S. National Museum of Natural History (Smithsonian Institution), catalog number NMNH168696, and the Natural History Museum, London, catalog number BM1980,539.

In the ensuing study, reported herein, we conducted EMPA on the Otto Mountain unknown and both of the schieffelinite cotypes and single-crystal structure analyses on the Otto Mountain unknown and the NMNH schieffelinite cotype. Our determination is that the unknown yellow crystals from Otto Mountain represent the chromate analog of schieffelinite and, consequently, we have chosen to name the new mineral chromschieffelinite. The new mineral and name have been approved by the Commission on New Minerals, Nomenclature and Classification of the Interna-

* E-mail: akampf@nhm.org

0003-004X/12/0001–212$05.00/DOI: http://dx.doi.org/10.2138/am.2011.3909

tional Mineralogical Association (IMA 2011-003). One holotype specimen (consisting of two pieces) is deposited in the Natural History Museum of Los Angeles County, catalog number 63511.

Occurrence

Chromschieffelinite was discovered at the Bird Nest drift (35°16.606′N, 116° 05.956′W) on the southwest flank of Otto Mountain, 0.4 miles northwest of the Aga mine. Chromschieffelinite is, so far, the rarest of the new minerals from Otto Mountain, only occurring on one mineral specimen. The only material available is from a single 1 mm diameter vug in a quartz vein. Other species identified on the holotype specimen are: chalcopyrite, chrysocolla, galena, goethite, hematite, khinite, pyrite, and wulfenite. Other species identified in the mineral assemblages at Otto Mountain are outlined in detail in Housley et al. (2011). Chromschieffelinite occurs as a secondary, oxidation zone mineral and is presumed to have formed by oxidation of tellurides and galena. The source of the Cr is not clear, although two other secondary chromates, fornacite and vauquelinite, have been found in the Bird Nest drift mineral assemblage.

Physical and optical properties

Chromschieffelinite crystals (Fig. 1) are blocky to tabular on {010} with striations parallel to [001] and are up to 0.2 mm in maximum dimension. The crystal forms measured on a two-circle reflecting goniometer are {010}, {210}, {120}, {150}, {180}, {212}, and {101} (Fig. 2). No twinning was observed optically under crossed polars or based upon single-crystal X-ray diffraction. The color and streak are pale yellow and the luster is adamantine. The Mohs hardness is estimated at 2. The new mineral is brittle with irregular fracture and one perfect cleavage on {010}. The density could not be measured because it is greater than those of available high-density liquids and there is insufficient material for physical measurement. The calculated density based on the ideal formula is 5.892 g/cm^3. Insufficient material was available for testing the reactivity in acid; however, by analogy to schieffelinite, chromschieffelinite is expected to be readily soluble in cold dilute HCl or HNO_3.

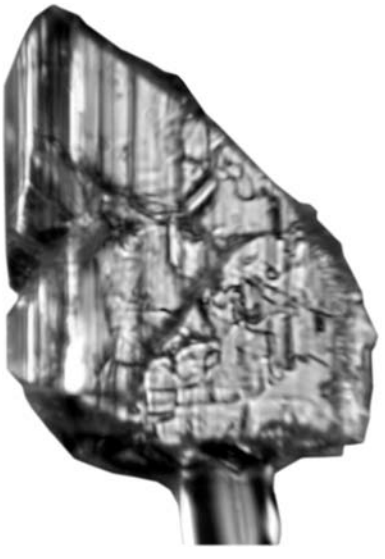

Figure 1. Tabular crystal of chromschieffelinite, 140 × 110 × 35 μm, used in optical and morphological studies. The crystal is tabular on {010} and striated parallel to [001]. Note that right side of the crystal is bounded by broken surfaces rather than faces.

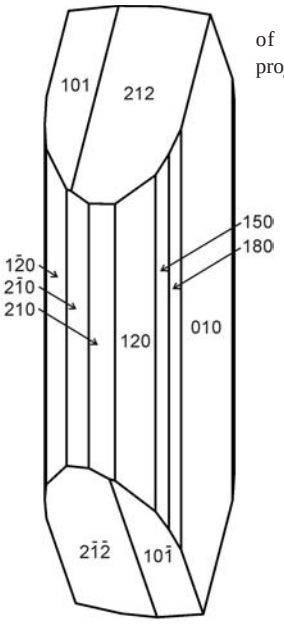

Figure 2. Idealized crystal drawing of chromschieffelinite (clinographic projection in standard orientation).

Crystals of chromschieffelinite are biaxial (–) with the indices of refraction: $\alpha = 1.930(5)$, $\beta = 1.960(5)$, and $\gamma = 1.975(5)$, measured in white light. The $2V$, measured directly on a spindle stage, is 68(2)°, while the calculated $2V$ is 69.6°. The dispersion is $r < v$, strong, orientation is X = **b**, Y = **c**, Z = **a**. No pleochroism was observed.

Chemical composition

Chemical analyses of chromschieffelinite and the Smithsonian Institution (NMNH) schieffelinite cotype (NMNH168696) were carried out using a JEOL8200 electron microprobe (WDS mode, 15 kV, 5 nA, and 20 μm beam diameter) at the Division of Geological and Planetary Sciences, California Institute of Technology. The standards used were: PbS (Pb), Te metal (Te), anorthite (Al), anhydrite (S), and Cr_2O_3 (Cr). Chemical analyses of the Natural History Museum, London (NHM), schieffelinite cotype (BM1980,539) were carried out using a Cameca SX100 electron microprobe (WDS mode, 15 kV, 10 nA, and 20 μm beam diameter) at the Mineralogy Department, Natural History Museum, London. The standards used were: vanadinite (Pb), bismuth telluride (Te), and celestine (S). Analytical results are given in Table 1. For chromschieffelinite, S was analyzed for, but was always below the detection limit (0.1 wt% S). No other elements were detected in EDS analyses in any of the samples.

There were insufficient quantities for CHN analyses, so in each case H_2O was calculated on the basis of Te = 6, charge balance, and 43 O apfu (34 framework and 9 channel), as determined by crystal structure analyses (see below). Note that chromschieffelinite is prone to electron beam damage, which contributes to the low analytical totals. This is a common feature observed in many other tellurate minerals (e.g., Kampf et al. 2010a–2010g;

TABLE 1. Chemical analytical data for chromschieffelinite and schieffelinite

	Chromschieffelinite* EMPA (4 analyses)			Schieffelinite (NMNH168696) EMPA (5 analyses)			Schieffelinite (BM1980,539) EMPA (7 analyses)			Schieffelinite (Williams 1980) wet chemistry
	wt%	range	SD	wt%	range	SD	wt%	range	SD	wt%
PbO	59.42	59.01–59.81	0.42	63.65	64.45–62.88	0.62	63.94	63.21–64.99	0.58	58.2
Al_2O_3				0.13	0.02–0.37	0.14				
TeO_3	29.08	29.00–29.12	0.05	29.30	28.14–29.93	0.82	30.55	30.47–30.65	0.07	28.6
CrO_3	1.86	1.67–2.08	0.21							
SO_3				1.21	1.05–1.42	0.17	2.19	2.04–2.32	0.10	6.8
H_2O	6.63			6.83			6.42			4.7
Total	96.99			101.12			103.10			98.3

* The EMP for chromschieffelinite normalized to 100% is PbO 61.27, TeO_3 29.98, CrO_3 1.91, H_2O 6.84, Total 100 wt%.

Mills et al. 2009, 2010).

The empirical formulas (based on Te+Al = 6) are

Chromschieffelinite:

$Pb_{9.65}Te_6O_{19.96}(OH)_{14.04}(CrO_4)_{0.67}(H_2O)_{6.32}$

Schieffelinite (NMNH168696):

$Pb_{10.10}(Te_{5.91}Al_{0.09})_{\Sigma 6}O_{20.82}(OH)_{13.18}(SO_4)_{0.54}(H_2O)_{6.84}$

Schieffelinite (BM1980,539):

$Pb_{9.88}Te_6O_{20.62}(OH)_{13.38}(SO_4)_{0.94}(H_2O)_{5.06}$.

The simplified formula for the minerals is: $Pb_{10}Te_6O_{22-2x}(OH)_{12+2x}(TO_4)_x(H_2O)_{9-4x}$, where T = Cr or S and, based upon our EMP analyses (all analyses, not just the averages), x is variable from 0.46 to 1.00. The upper end of this range (x = 1) is taken as the ideal value. Therefore, the ideal formulas are: chromschieffelinite, $Pb_{10}Te_6O_{20}(OH)_{14}(CrO_4)(H_2O)_5$, which requires PbO 61.97, TeO_3 29.25, CrO_3 2.78, H_2O 6.00, total 100 wt% and schieffelinite, $Pb_{10}Te_6O_{20}(OH)_{14}(SO_4)(H_2O)_5$, which requires PbO 62.31, TeO_3 29.41, SO_3 2.24, H_2O 6.04, total 100 wt%.

It is important to note that the wet chemical analysis reported by Williams (1980), and the formula, $Pb_8(TeO_4)_5(SO_4)_3(H_2O)_8$, do not match our EMP analyses of schieffelinite on the two cotype specimens studied, particularly with respect to the amount of S. It also does not fit the crystal structure (see below). Wet chemical analyses, because they are conducted on bulk samples, are commonly compromised by impurity phases. In this case, we suspect contamination from an associated sulfate-rich phase, possibly anglesite. Further evidence that supports this interpretation is that

TABLE 2. X-ray powder diffraction data for chromschieffelinite; d_{calc} and I_{calc} were calculated from the crystal structure using JADE 9.1

I_{obs}	d_{obs}	d_{calc}	I_{calc}	$h\,k\,l$	I_{obs}	d_{obs}	d_{calc}	I_{calc}	$h\,k\,l$
100	9.814(5)	9.7481	100	0 2 0			2.1203	3	4 4 1
8	8.64(4)	8.6591	4	1 1 0	15	2.083(2)	2.0862	5	2 4 4
19	7.196(5)	7.1472	17	0 2 1	33	2.040(3)	2.0427	10	1 1 5
5	6.74(2)	6.6830	3	1 1 1			2.0261	9	3 5 3
7	4.87(1)	4.8741	2	0 4 0	6	2.002(1)	2.0016	5	4 4 2
		4.8323	2	2 0 0			2.0006	2	0 8 3
2	4.556(3)	4.4925	5	1 1 2	28	1.9576(9)	1.9611	3	1 9 2
22	4.38(1)	4.3905	6	2 0 1			1.9585	7	1 3 5
		4.3295	4	2 2 0			1.9496	3	0 10 0
5	4.00(3)	4.0032	3	2 2 1			1.9488	3	4 2 3
9	3.778(4)	3.7637	6	1 3 2			1.9430	4	3 3 4
41	3.575(1)	3.5736	13	0 4 2	18	1.907(2)	1.9067	8	4 6 1
		3.5570	20	2 0 2			1.8818	3	2 6 4
25	3.436(1)	3.4316	13	2 4 0	21	1.8221(8)	1.8246	4	5 3 1
		3.4193	20	1 5 1			1.8190	4	4 6 2
44	3.347(3)	3.3415	20	2 2 2	20	1.7838(4)	1.8056	3	3 7 3
53	3.262(1)	3.2621	14	2 4 1			1.7818	5	2 10 1
		3.2494	6	0 6 0			1.7785	9	4 0 4
		3.2476	28	1 1 3	7	1.7500(7)	1.7496	3	4 2 4
45	3.0522(6)	3.0424	37	3 1 1			1.7473	2	5 3 2
55	2.9455(6)	2.9789	11	1 5 2	13	1.7122(6)	1.7097	5	2 10 2
		2.9379	37	1 3 3			1.7088	3	5 5 1
17	2.883(2)	2.8733	15	2 4 2			1.6934	3	4 8 1
22	2.7822(8)	2.7833	12	3 3 1	33	1.6500(2)	1.6546	5	1 11 2
		2.7637	11	0 6 2			1.6531	3	1 7 5
21	2.701(2)	2.6964	9	2 6 0			1.6468	4	2 0 6
		2.6763	5	1 7 0			1.6448	3	5 5 2
23	2.6113(7)	2.6119	12	2 6 1			1.6437	10	3 7 4
		2.5935	10	1 7 1	2	1.61(2)	1.6238	3	2 2 6
10	2.5223(9)	2.5299	2	3 3 2			1.6108	2	6 0 0
		2.5161	2	1 5 3	8	1.600(9)	1.6045	2	3 5 5
		2.5143	5	1 1 4			1.5917	3	0 8 5
22	2.370(1)	2.3848	5	1 7 2	13	1.564(2)	1.5657	1	0 10 4
		2.3740	3	0 8 1			1.5608	2	1 11 3
		2.3621	4	1 3 4			1.5602	2	2 4 6
		2.3547	4	4 0 1			1.5601	1	4 6 4
7	2.232(3)	2.2462	1	2 2 4	7	1.5199(7)	1.5237	3	2 12 1
		2.2454	1	3 5 2			1.5201	3	5 7 2
		2.2277	2	3 3 3	9	1.4844(6)	1.5017	3	4 10 1
18	2.1328(7)	2.1308	3	2 8 1			1.4836	3	3 9 4
		2.1267	4	1 7 3					

the Gladstone-Dale compatibility index (Mandarino 1981) for the chemistry, average index of refraction (1.926) and calculated density (5.15) reported by Williams (1980) is –0.14 (poor), while that for our chemistry (for NMNH168696), calculated density (5.987) and Williams' average index of refraction is 0.027 (excellent). We also believe it likely that the density measurement by Williams (1980) using a Berman balance, 4.98(12) g/cm^3, was conducted on an impure or porous sample. The Gladstone-Dale compatability index for chromschieffelinite is 0.004 (superior).

X-RAY CRYSTALLOGRAPHY AND STRUCTURE DETERMINATIONS

All powder and single-crystal X-ray diffraction data were obtained on a Rigaku R-Axis Rapid II curved imaging plate microdiffractometer utilizing monochromatized Mo*K*α radiation. For chromschieffelinite observed powder *d*-spacings (with standard deviations) and intensities were derived by profile fitting using JADE 9.1 software. Data (in angstroms for Mo*K*α) are given in Table 2 (see previous page). Unit-cell parameters refined from the powder data using JADE 9.1 with whole pattern fitting are: a = 9.670(3), b = 19.521(6), c = 10.524(3) Å, and V = 1986.6(9) Å^3. The observed powder data fit well with those calculated from the structure. The relatively low precision of the cell refined from the powder data is attributable to the use of Mo*K*α radiation.

The Rigaku CrystalClear software package was used for processing of the diffraction data, including the application of an empirical absorption correction. The significantly higher R_{int} for schieffelinite compared to chromschieffelinite, 0.0984 vs. 0.0512, is probably more attributable to the quality of the data than to the ability of the software to correct for the absorption effects. The schieffelinite diffraction frames exhibited noticeably less sharp diffraction spots. The structures were solved by direct methods using SIR92 (Altomare et al. 1994). The SHELXL-97 software (Sheldrick 2008) was used for the refinement of the structure. Details of the data collections and structure refinements for schieffelinite (NMNH168696) and chromschieffelinite are provided in Table 3. Fractional coordinates and atomic displacement parameters are provided in Table 4, selected interatomic distances in Table 5, and bond valences in Table 6.

DESCRIPTION OF THE STRUCTURE

The structures of schieffelinite and chromschieffelinite contain two types of $Te^{6+}O_6$ octahedra. The Te1 octahedra are isolated, while the Te2 octahedra are joined into $Te_2^{6+}O_{11}$ dimers by corner-sharing. Both types of octahedra are linked into a three-dimensional framework via bonds to three different Pb^{2+} atoms. The framework has large channels along **c**, which contain disordered SO_4 or CrO_4 groups and H_2O (Fig. 3). Each of the three Pb^{2+} coordinations include bonds to $Te^{6+}O_6$ octahedra, as well as to channel O atoms. The lone-electron pair of each Pb^{2+} is stereochemically active, resulting in one-sided Pb-O coordination arrangements. The short Pb-O bonds of the Pb^{2+} coordinations are all to $Te^{6+}O_6$ octahedra, resulting in strongly bonded layers parallel to {010}. The longer Pb-O bonds are to channel O atoms and to $Te^{6+}O_6$ octahedra in adjacent layers (Fig. 4). The layered nature of the structure is responsible for the perfect {010} cleavage.

The bond-valence analysis (Table 6) makes the assignment of O, OH, and H_2O sites in the framework straightforward (see last column of Table 6), except for the O7 site, which has

TABLE 3. Data collection and structure refinement details for schieffelinite and chromschieffelinite

	Schieffelinite	Chromschieffelinite
Diffractometer	Rigaku R-Axis Rapid II	Rigaku R-Axis Rapid II
X-ray radiation	Mo*K*α (λ = 0.71075 Å)	Mo*K*α (λ = 0.71075 Å)
Temperature	298(2) K	298(2) K
Structural Formula	$Pb_{10}Te_6O_{20}(OH)_{14}(SO_4)(H_2O)_5$	$Pb_{10}Te_6O_{20}(OH)_{14}(CrO_4)(H_2O)_5$
Space group	$C222_1$	$C222_1$
Unit-cell dimensions	a = 9.6581(3) Å	a = 9.6646(3) Å
	b = 19.5833(7) Å	b = 19.4962(8) Å
	c = 10.5027(7) Å	c = 10.5101(7) Å
Z	2	2
Volume	1986.45(16) Å^3	1980.33(17) Å^3
Density (for above formula)	6.055 g cm^{-3}	6.040 g cm^{-3}
Absorption coefficient	46.7 mm^{-1}	47.1 mm^{-1}
F(000)	3064	3048
Crystal size	70 × 70 × 5 µm	80 × 55 × 10 µm
θ range	3.0 to 25.03°	2.8 to 25.01°
Index ranges	$-11 \le h \le 11$	$-11 \le h \le 10$
	$-23 \le k \le 23$	$-23 \le k \le 21$
	$-12 \le l \le 12$	$-12 \le l \le 12$
Reflections collected/unique	10934/1746 [R_{int} = 0.0984]	9151/1731 [R_{int} = 0.0512]
Reflections with $F_o > 4\sigma F$	1624	1681
Completeness to θ_{max}	99.7%	98.9%
Max. and min. transmission	0.8000 and 0.1375	0.6504 and 0.1168
Refinement method	Full-matrix least-squares on F^2	Full-matrix least-squares on F^2
Parameters refined	142	142
GoF	0.852	1.039
Final R indices [$F_o > 4\sigma F$]	R_1 = 0.0282, wR_2 = 0.0589	R_1 = 0.0277, wR_2 = 0.0610
R indices (all data)	R_1 = 0.0309, wR_2 = 0.0600	R_1 = 0.0289, wR_2 = 0.0615
Largest diff. peak/hole	+1.22/–1.01 e Å^{-3}	+2.57/–1.53 e Å^{-3}
Flack parameter	0.014(8)	0.021(7)

$R_{int} = \Sigma|F_o^2 - F_o^2(\text{mean})|/\Sigma[F_o^2]$; GoF = $S = \{\Sigma[w(F_o^2 - F_c^2)^2]/(n-p)\}^{1/2}$; $R_1 = \Sigma||F_o| - |F_c||/\Sigma|F_o|$; $wR_2 = \{\Sigma[w(F_o^2 - F_c^2)^2]/\Sigma[w(F_o^2)^2]\}^{1/2}$; $w = 1/[\sigma^2(F_o^2) + (aP)^2]$ where P is $[2F_c^2 + \text{Max}(F_o^2,0)]/3$; for schieffelinite a is 0 and b is 0; for chromschieffelinite a is 0.0229 and b is 0.

TABLE 4. Fractional coordinates and atomic displacement parameters for schieffelinite and chromschieffelinite*

	x/a	*y/b*	*z/c*	U_{eq}	U_{11}	U_{22}	U_{33}	U_{23}	U_{13}	U_{12}
Schieffelinite										
Pb1	0.5000	0.73650(4)	0.2500	0.0318(2)	0.0276(4)	0.0239(4)	0.0440(6)	0.000	0.0057(4)	0.000
Pb2	0.85073(5)	0.65799(3)	0.37439(6)	0.02931(16)	0.0267(3)	0.0246(3)	0.0366(3)	–0.0003(3)	0.0054(3)	–0.0003(3)
Pb3	0.78502(6)	0.84797(3)	0.49090(6)	0.03594(18)	0.0603(4)	0.0240(3)	0.0235(3)	0.0030(3)	–0.0084(3)	–0.0046(3)
Te1	0.5000	0.55838(6)	0.2500	0.0198(3)	0.0258(7)	0.0174(6)	0.0164(7)	0.000	0.0006(6)	0.000
Te2	0.84780(9)	0.79060(4)	0.15087(9)	0.0179(2)	0.0164(4)	0.0193(5)	0.0179(5)	0.0005(4)	–0.0018(4)	–0.0008(4)
O1	0.6317(10)	0.6271(4)	0.2089(8)	0.024(2)	0.027(5)	0.022(5)	0.023(5)	0.012(4)	–0.001(4)	–0.005(4)
O2	0.5713(10)	0.5540(5)	0.4240(9)	0.029(2)	0.039(6)	0.027(6)	0.022(6)	–0.001(5)	–0.006(5)	–0.004(5)
O3	0.3724(10)	0.4866(5)	0.2976(10)	0.039(3)	0.043(6)	0.034(6)	0.041(7)	–0.010(5)	–0.003(5)	–0.020(5)
O4	0.9163(8)	0.7005(4)	0.1304(9)	0.023(2)	0.013(4)	0.025(5)	0.030(6)	0.002(5)	0.000(4)	–0.003(4)
O5	0.8153(8)	0.7347(5)	0.5610(8)	0.021(2)	0.015(5)	0.029(5)	0.019(5)	0.003(4)	0.004(4)	–0.005(4)
O6	0.7653(10)	0.7637(5)	0.3071(8)	0.023(2)	0.029(6)	0.026(5)	0.015(5)	0.001(4)	–0.005(4)	0.004(5)
O7	0.5580(9)	0.6813(5)	0.4976(10)	0.024(2)	0.026(5)	0.029(5)	0.018(5)	–0.003(5)	–0.002(4)	0.000(4)
O8	0.0000	0.8279(6)	0.2500	0.029(3)	0.020(7)	0.021(7)	0.046(9)	0.000	–0.022(7)	0.000
O9	0.7676(9)	0.8815(5)	0.1632(10)	0.026(2)	0.021(5)	0.022(5)	0.037(7)	0.004(4)	–0.002(5)	0.004(4)
S	0.0640(16)	0.5036(10)	0.4652(15)	0.044(5)						
O10	0.214(3)	0.5000	0.5000	0.067(11)						
O11	0.488(5)	0.9372(17)	0.045(5)	0.19(2)						
O12	0.046(8)	0.526(4)	0.329(4)	0.10(3)						
OW1	–0.114(6)	0.5000	0.5000	0.14(2)						
OW2	0.482(3)	0.8803(13)	0.179(2)	0.055(7)						
OW3	0.097(4)	0.534(2)	0.360(4)	0.112(16)						
Chromschieffelinite										
Pb1	0.5000	0.73669(4)	0.2500	0.02636(18)	0.0210(4)	0.0188(4)	0.0393(4)	0.000	0.0048(3)	0.000
Pb2	0.85091(5)	0.65778(3)	0.37381(4)	0.02338(14)	0.0188(3)	0.0200(3)	0.0314(2)	0.0018(2)	0.0048(2)	–0.0010(2)
Pb3	0.78519(6)	0.84795(3)	0.49042(4)	0.03141(16)	0.0551(4)	0.0189(3)	0.0202(2)	0.0037(2)	–0.0102(2)	–0.0062(3)
Te1	0.5000	0.55833(6)	0.2500	0.0149(2)	0.0183(6)	0.0134(6)	0.0131(5)	0.000	–0.0005(4)	0.000
Te2	0.84797(8)	0.79074(4)	0.15086(6)	0.01206(16)	0.0096(3)	0.0139(4)	0.0127(3)	0.0003(3)	–0.0015(3)	–0.0005(3)
O1	0.6286(9)	0.6271(4)	0.2077(6)	0.0170(19)	0.020(5)	0.011(4)	0.020(4)	0.000(3)	0.003(3)	0.006(4)
O2	0.5707(10)	0.5544(5)	0.4228(7)	0.028(2)	0.032(6)	0.029(6)	0.023(4)	–0.002(4)	–0.010(4)	–0.003(5)
O3	0.3728(11)	0.4860(5)	0.2998(8)	0.034(2)	0.053(7)	0.013(5)	0.036(5)	–0.002(4)	–0.001(4)	–0.014(5)
O4	0.9161(8)	0.6999(4)	0.1306(7)	0.0181(18)	0.010(4)	0.014(5)	0.030(4)	0.004(4)	–0.001(3)	0.005(4)
O5	0.8150(9)	0.7336(4)	0.5598(6)	0.0152(19)	0.026(5)	0.005(4)	0.014(3)	0.003(3)	0.008(3)	0.003(3)
O6	0.7655(8)	0.7640(4)	0.3088(6)	0.0137(17)	0.010(4)	0.020(5)	0.011(3)	0.004(3)	0.004(3)	0.000(4)
O7	0.5579(9)	0.6818(5)	0.4978(7)	0.023(2)	0.023(5)	0.023(5)	0.022(4)	–0.002(4)	–0.011(4)	–0.002(4)
O8	0.0000	0.8272(6)	0.2500	0.021(3)	0.008(6)	0.021(7)	0.033(6)	0.000	–0.011(5)	0.000
O9	0.7667(9)	0.8820(5)	0.1633(7)	0.0204(19)	0.016(5)	0.022(5)	0.023(4)	0.004(3)	–0.004(3)	0.003(4)
Cr	0.0584(13)	0.5030(7)	0.4555(8)	0.050(3)						
O10	0.221(3)	0.5000	0.5000	0.072(11)						
O11	0.516(5)	0.9325(16)	0.050(3)	0.130(15)						
O12	0.054(5)	0.538(2)	0.313(3)	0.033(9)						
OW1	–0.139(7)	0.5000	0.5000	0.14(2)						
OW2	0.480(3)	0.8803(17)	0.176(2)	0.078(9)						
OW3	0.124(4)	0.532(2)	0.386(3)	0.102(11)						

* Site occupancies (fixed): S: 0.25, Cr: 0.25, O10: 0.5, O11: 0.5, O12: 0.25, OW1: 0.5, OW2: 0.5, OW3: 0.5.

TABLE 5. Selected bond lengths (Å) in schieffelinite and chromschieffelinite

	Schieffelinite	Chromschieffelinite		Schieffelinite	Chromschieffelinite
Pb1-O1 (×2)	2.529(9)	2.512(8)	Pb3-O7	2.700(9)	2.701(9)
Pb1-O6 (×2)	2.685(9)	2.692(8)	Pb3-O10	3.057(6)	3.031(6)
Pb1-O5 (×2)	2.728(9)	2.744(8)	Pb3-OW3	3.33(4)	3.10(4)
Pb1-O7 (×2)	2.872(10)	2.871(8)	Pb3-OW2	3.19(2)	3.17(3)
Pb1-OW2 (×2)	2.92(2)	2.91(3)	Pb3-O8	3.297(2)	3.295(2)
<Pb1-O>	2.75	2.728	Pb3-O11	3.19(5)	3.37(5)
Pb2-O6	2.339(9)	2.331(8)	Pb3-O3	3.493(10)	3.461(9)
Pb2-O4	2.399(8)	2.397(8)	Pb3-O2	3.483(10)	3.474(10)
Pb2-O5	2.493(9)	2.475(7)	Pb3-O9	3.508(10)	3.506(8)
Pb2-O4	2.768(10)	2.758(8)	<Pb3-O>	3.02	3.01
Pb2-O1	2.804(9)	2.833(8)	Te1-O1 (×2)	1.902(9)	1.881(8)
Pb2-O11	3.02(5)	2.87(3)	Te1-O3 (×2)	1.936(10)	1.942(9)
Pb2-O12	3.24(8)	3.13(4)	Te1-O2 (×2)	1.954(9)	1.942(8)
Pb2-O7	3.143(9)	3.153(9)	<Te1-O>	1.931	1.922
Pb2-O12	3.50(5)	3.19(3)	Te2-O4	1.897(9)	1.902(8)
Pb2-O9	3.332(10)	3.339(8)	Te2-O5	1.903(8)	1.903(8)
Pb2-OW1	3.381(6)	3.351(2)	Te2-O6	1.898(9)	1.914(7)
Pb2-O2	3.421(10)	3.415(10)	Te2-O7	1.929(10)	1.924(8)
Pb2-OW3	3.40(4)	3.60(4)	Te2-O8	1.944(5)	1.937(4)
Pb2-OW2	3.66(3)	3.65(3)	Te2-O9	1.947(9)	1.949(9)
Pb2-OW3	3.50(4)	3.67(4)	<Te2-O>	1.920	1.922
<Pb2-O>	3.09	3.06	S/Cr-O11	1.40(3)	1.55(2)
Pb3-O5	2.355(9)	2.364(8)	S/Cr-O10	1.49(2)	1.64(2)
Pb3-O1	2.475(9)	2.479(7)	S/Cr-O12	1.50(3)	1.64(2)
Pb3-O6	2.547(9)	2.522(8)	S/Cr-O11	1.52(3)	1.76(2)
Pb3-O4	2.613(9)	2.613(8)	<S/Cr-O>	1.48	1.65

TABLE 6. Bond valence sums for schieffelinite and chromschieffelinite

	Pb1	Pb2	Pb3	Te1	Te2	S	Σ	
				Schieffelinite				
O1	0.32 ×2↓	0.18	0.35	1.04 ×2↓			1.89	O
O2		0.05	0.04	0.90 ×2↓			0.99	OH
O3			0.04	0.95 ×2↓			0.99	OH
O4		0.41,0.19	0.27		1.06		1.93	O
O5	0.21 ×2↓	0.34	0.45		1.04		2.04	O
O6	0.23 ×2↓	0.46	0.30		1.05		2.04	O
O7	0.16 ×2↓	0.09	0.22		0.97		1.44	O,OH
O8			0.07 ×2→		0.93 ×2↓		2.00	O
O9		0.06	0.04		0.92		1.02	OH
O10			0.05 ×4→			1.44	1.54	O
O11		0.06 ×2→	0.04 ×2→			1.84 ×½→	1.68	O
						1.12 ×½→		
O12		0.02 ×4→				1.40	1.43	O
		0.01 ×4→						
OW1		0.03 ×4→					0.06	H_2O
OW2	0.08 ×2↓→	0.02 ×2→	0.04 ×2→				0.14	H_2O
OW3		0.03 ×2→	0.03 ×2→				0.08	H_2O
		0.02 ×2→						
Σ	2.00	1.97	1.94	5.78	5.97	6.00		
				Chromschieffelinite				
O1	0.33 ×2↓	0.17	0.35	1.10 ×2↓			1.95	O
O2		0.05	0.05	0.93 ×2↓			1.03	OH
O3			0.05	0.93 ×2↓			0.98	OH
O4		0.41,0.20	0.27		1.04		1.92	O
O5	0.20 ×2↓	0.35	0.44		1.04		2.03	O
O6	0.23 ×2↓	0.47	0.32		1.01		2.03	O
O7	0.16 ×2↓	0.02	0.22		0.98		1.38	O,OH
O8			0.03 ×2→		0.95 ×2→		1.96	O
O9		0.06	0.04		0.92		1.02	OH
O10			0.06 ×4→			1.52	1.76	O
O11		0.08 ×2→	0.03 ×2→			1.93 ×½→	1.74	O
						1.10 ×½→		
O12		0.02 ×4→				1.52	1.69	O
		0.02 ×4→						
OW1		0.03 ×4→					0.12	H_2O
OW2	0.07 ×2↓→	0.02 ×2→	0.04 ×2→				0.26	H_2O
OW3		0.02 ×2→	0.05 ×2→				0.18	H_2O
		0.02 ×2→						
Σ	1.98	2.01	1.95	5.92	5.94	6.06		

Notes: Multiplicity is indicated by ×↓→; Pb^{2+}-O bond strengths from Krivovichev and Brown (2001); Te^{6+}-O, Sr^{6+}-O, and Cr^{6+}-O bond strengths from Brown and Altermatt (1985).

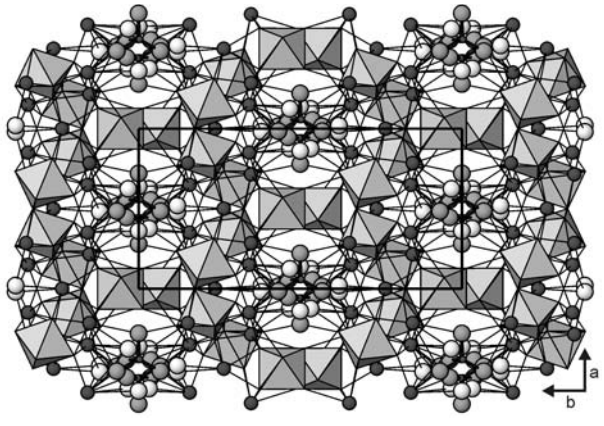

FIGURE 3. Structure of chromschieffelinite viewed down **c**, the channel direction. TeO_6 octahedra are shown in gray. Atoms shown as spheres are: Pb = large dark gray, O of H_2O = large white, O of CrO_4 group = large light gray, and Cr = small dark gray. The unit cell is outlined by a thick black line. For a clearer view of the bonding in the channels, see Figures 5 and 6.

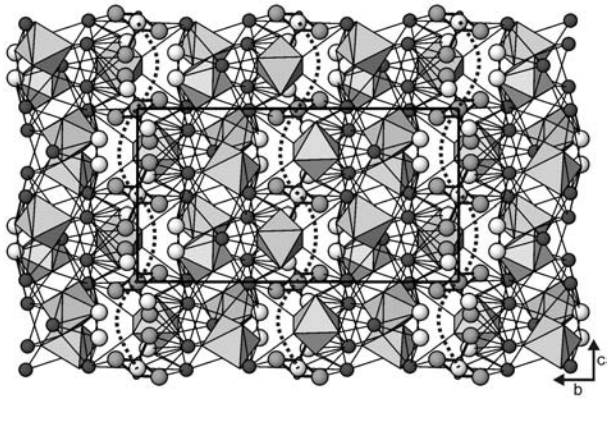

FIGURE 4. Structure of chromschieffelinite viewed down **a**. Dotted lines indicate the boundaries between the more strongly bonded {010} layers. Other components of the structure are the same as in Figure 3.

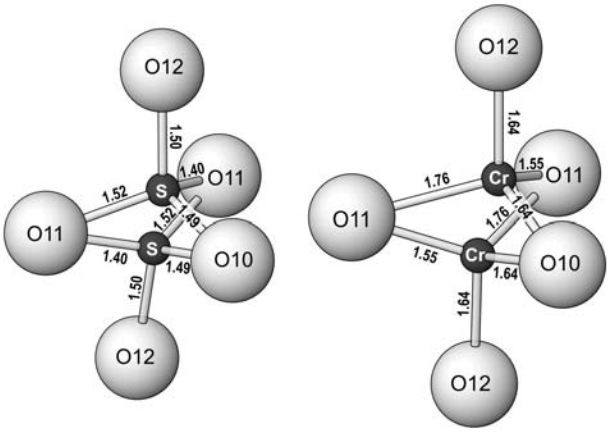

FIGURE 5. The disordered SO_4 group in schieffelinite (**left**) and CrO_4 group in chromschieffelinite (**right**).

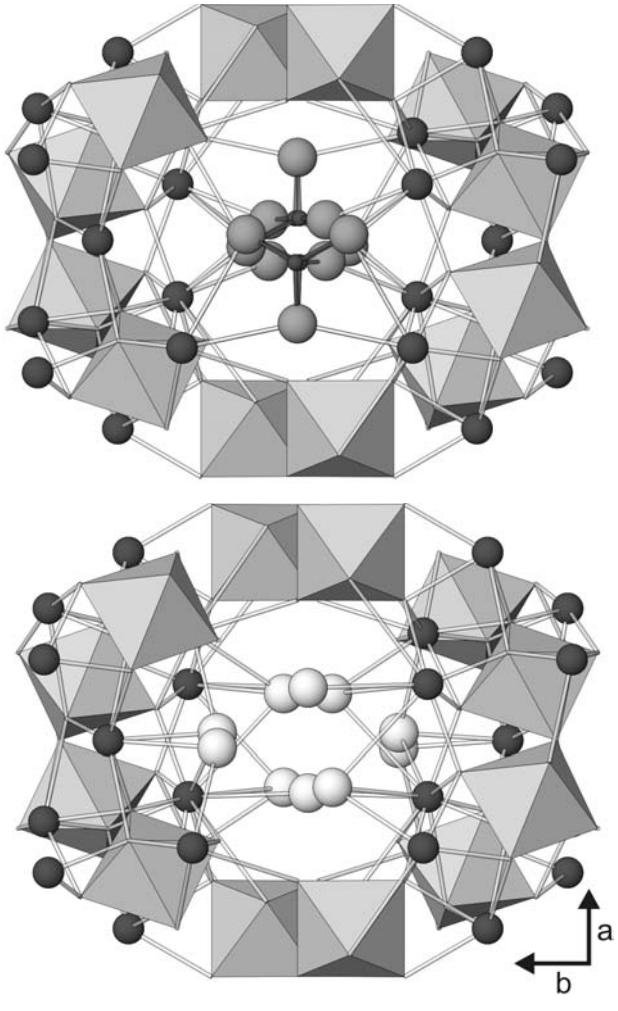

FIGURE 6. The channel in the chromschieffelinite structure containing only CrO_4 groups (**top**) and only H_2O (**bottom**).

a bond-valence sum that is rather high for an OH site. This suggests that the site has mixed O/OH character. The ideal formula is consistent with this site being half O and half OH. Note that the bond-valence analysis does not take hydrogen bonding into consideration.

There are seven partially occupied sites in the channel of each structure. Based upon geometry, a grouping of four sites, S/Cr, O10, O11, and O12, is identified as a SO_4 (or CrO_4) group in two alternative configurations, each sharing the same triangular O11-O10-O11 base. The partially occupied S/Cr site is placed on either side of the triangular base and apical O12 sites complete the tetrahedral coordination (Fig. 5).

The refined occupancies of the channel sites in the structures of both schieffelinite and chromschieffelinte are consistent with a structure in which the channels are occupied approximately half of the time with SO_4/CrO_4 tetrahedra (in one of the two possible orientations) and half of the time with three H_2O sites, OW1, OW2, and OW3. Figure 6 shows the channel in the chromschieffelinite structure, in one case occupied only with CrO_4 tetrahedra and in the other occupied only with H_2O. However, this clearly is an overly simplified way to model the structures and in reality it is clear that a SO_4 or CrO_4 tetrahedron in one of the two orientations will share the channel with nearby H_2O molecules. Hydrogen bonding between the H_2O and SO_4 or CrO_4 groups must help to balance the otherwise low bond-valence sums of the tetrahedral O atoms.

In the final refinements for each structure, the S-O and Cr-O bond lengths were constrained to 1.450 and 1.644 Å, respectively, and the seven channel sites were fixed at the occupancies corresponding to the channels being half occupied by SO_4/CrO_4 tetrahedra and half occupied by H_2O. Note that, for the SO_4 and CrO_4 tetrahedra, the occupancies of the O10 and O11 sites, shared between the two alternate tetrahedral configurations, have occupancies of ½, while the S/Cr and O12 sites have occupancies of ¼. Also, note that the large variation in Cr-O and S-O bond lengths is probably an artifact of the disorder rather than a reflection of actual tetrahedral distortion.

Finally, it should be noted that the electron microprobe analyses for the crystals of schieffelinite and chromschieffelinite taken from the same specimens as the crystals used in the structure studies showed significantly less S and Cr than the amounts suggested by the structure studies, while the EMPA conducted on a different schieffelinite cotype (BM1980,539) provides close to the "ideal" amount of S suggested by the structure. While S or Cr content may be highly variable from crystal to crystal on the same specimen, only moderate variability is suggested by the EMPAs (see Table 1). A more likely explanation is that the sites ascribed to the SO_4 and CrO_4 groups in the structure analyses may in part be O atoms of H_2O groups.

ACKNOWLEDGMENTS

The paper benefited from comments by reviewer Joël Brugger, Associate Editor G. Diego Gatta, and Technical Editor Ron Petersen. John Dagenais is thanked for providing the holotype specimen of chromschieffelinite. Paul Powhat (NMNH) is thanked for providing one of the cotype specimens of schieffelinite for study. The Caltech EMP analyses were supported by a grant from the Northern California Mineralogical Association. The remainder of this study was funded by the John Jago Trelawney Endowment to the Mineral Sciences Department of the Natural History Museum of Los Angeles County.

REFERENCES CITED

Altomare, A., Cascarano, G., Giacovazzo, C., Guagliardi, A., Burla, M.C., Polidori, G., and Camalli, M. (1994) SIR92—a program for automatic solution of crystal structures by direct methods. Journal of Applied Crystallography, 27, 435.

Brown, I.D. and Altermatt, D. (1985) Bond-valence parameters from a systematic analysis of the inorganic crystal structure database. Acta Crystallographica, B41, 244–247.

Housley, R.M., Kampf, A.R., Mills, S.J., Marty, J., and Thorne, B. (2011) The remarkable occurrence of rare secondary minerals at Otto Mountain near Baker, California – including seven new species. Rocks and Minerals, 86, 132–142.

Kampf, A.R., Housley, R.M., Mills, S.J., Marty, J., and Thorne, B. (2010a) Lead-tellurium oxysalts from Otto Mountain near Baker, California: I. Ottoite, Pb_2TeO_5, a new mineral with chains of tellurate octahedra. American Mineralogist, 95, 1329–1336.

Kampf, A.R., Marty, J., and Thorne, B. (2010b) Lead-tellurium oxysalts from Otto Mountain near Baker, California: II. Housleyite, $Pb_6CuTe_4TeO_{18}(OH)_2$, a new mineral with Cu-Te octahedral sheets. American Mineralogist, 95, 1337–1342.

Kampf, A.R., Housley, R.M., and Marty, J. (2010c) Lead-tellurium oxysalts from Otto Mountain near Baker, California: III. Thorneite, $Pb_6(Te_2O_{10})(CO_3)Cl_2(H_2O)$, the first mineral with edge-sharing octahedral dimers. American Mineralogist, 95, 1548–1553.

Kampf, A.R., Mills, S.J., Housley, R.M., Marty, J., and Thorne, B. (2010d) Lead-tellurium oxysalts from Otto Mountain near Baker, California: IV. Markcooperite, $Pb_2(UO_2)TeO_6$, the first natural uranyl tellurate. American Mineralogist, 95, 1554–1559.

Kampf, A.R., Mills, S.J., Housley, R.M., Marty, J., and Thorne, B. (2010e) Lead-tellurium oxysalts from Otto Mountain near Baker, California: V. Timroseite, $Pb_2Cu^{2+}_5(Te^{6+}O_6)_2(OH)_2$, and paratimroseite, $Pb_2Cu^{2+}_4(Te^{6+}O_6)_2(H_2O)_2$, new minerals with edge-sharing Cu-Te octahedral chains. American Mineralogist, 95, 1560–1568.

Kampf, A.R., Mills, S.J., Housley, R.M., Marty, J., and Thorne, B. (2010f) Lead-tellurium oxysalts from Otto Mountain near Baker, California: VI. Telluroperite, $Pb_3Te^{4+}O_4Cl_2$, the Te analogue of perite and nadorite. American Mineralogist, 95, 1569–1573.

Kampf, A.R., Mills, S.J., and Housley, R.M. (2010g) The crystal structure of munakataite, $Pb_2Cu_2(Se^{4+}O_3)(SO_4)(OH)_4$, from Otto Mountain, San Bernardino County, California, USA. Mineralogical Magazine, 74, 991–998.

Krivovichev, S.V. and Brown, I.D. (2001) Are the compressive effects of encapsulation an artifact of the bond valence parameters? Zeitschrift für Kristallographie, 216, 245–247.

Mandarino, J.A. (1981) The Gladstone-Dale relationship: Part IV. The compatability concept and its application. Canadian Mineralogist, 19, 441–450.

Mills, S.J., Kolitsch, U., Miyawaki, R., Groat, L.A., and Poirier, G. (2009) Joëlbruggerite, $Pb_3Zn_3(Sb^{5+},Te^{6+})As_2O_{13}(OH,O)$, the Sb^{5+} analogue of dugganite, from the Black Pine mine, Montana. American Mineralogist, 94, 1012–1017.

Mills, S.J., Kampf, A.R., Kolitsch, U., Housley, R.M., and Raudsepp, M. (2010) The crystal chemistry and crystal structure of kuksite, $Pb_3Zn_3Te^{6+}P_2O_{14}$, and a note on the crystal structure of yafsoanite, $(Ca,Pb)_3Zn(TeO_6)_2$. American Mineralogist, 95, 933–938.

Sheldrick, G.M. (2008) A short history of *SHELX*. Acta Crystallographica, A64, 112–122.

Williams, S. (1980) Schieffelinite, a new lead tellurate-sulphate from Tombstone, Arizona. Mineralogical Magazine, 43, 771–773.

MANUSCRIPT RECEIVED JUNE 8, 2011
MANUSCRIPT ACCEPTED AUGUST 14, 2011
MANUSCRIPT HANDLED BY G. DIEGO GATTA